Monatsh Chem (2009) 140:255–263
DOI 10.1007/s00706-008-0006-5

ORIGINAL PAPER

$B_{24}N_{24}$ nanocages: a GIAO density functional theory study of ^{14}N and ^{11}B nuclear magnetic shielding and electric field gradient tensors

Goudarz Mohseni Rouzbehani · Asadollah Boshra · Ahmad Seif

Received: 11 May 2008 / Accepted: 2 June 2008 / Published online: 12 September 2008

Abstract Density functional theory (DFT) calculations were performed to determine boron-11 and nitrogen-14 nuclear magnetic resonance (NMR) and nuclear quadrupole resonance (NQR) spectroscopy parameters in the three most stable $B_{24}N_{24}$ fullerenes for the first time. The considered samples were first allowed to relax entirely, and then the NMR and NQR calculations were performed on the geometrically optimized models. The calculations of the ^{11}B and ^{14}N nuclear magnetic shielding tensors and electric field gradient tensors employed the Gaussian 98 software implementation of the gauge-including atomic orbital (GIAO) method using the Becke3, Lee-Yang-Parr (B3LYP) DFT level and 6-311G** and 6-311++G** standard basis sets in each of the three optimized forms, and converted the results to experimentally measurable NMR parameters.The calculated NMR chemical shieldings of the three cages show significant differences, providing a way to identify these clusters. The evaluated NQR parameters of the ^{11}B and ^{14}N nuclei in the clusters are also reported and discussed.

Keywords Boron nitride nanocage · DFT · NMR · NQR · GIAO

G. M. Rouzbehani · A. Boshra · A. Seif
Department of Chemistry, Boroujerd Branch, Islamic Azad University, Imam Khomeini Campus, Yadegare Emam Street, Navvab Square, PO Box 518, 6915136111 Boroujerd, Lorestan, Iran

A. Boshra (✉)
Imam Khomeini Campus, Yadegare Emam Street, Navvab Square, PO Box 518, 6915136111 Boroujerd, Lorestan, Iran
e-mail: a.boshra@gmail.com

Introduction

Since the discovery of C_{60} fullerene in 1985 by Kroto et al. [1, 2], various carbon-based nanocage structures, such as fullerene clusters, nanotubes, nanocapsules, nanopolyhedrons, cones, cubes and onions, have been studied due to the great potential associated with the use of materials with low dimensions in an isolated environment [1, 3, 4]. Extensive research has been conducted both experimentally and theoretically on carbon nanotubes (CNTs) since their discovery via electron microscopy [3]. Many reports have appeared in the literature related to thermal [5] and structural studies that have shown a clear dependence of the propoerties of nanotubes on their diameter, length and chirality [6–8]. The structures and aromaticities of finite-length armchair [9] CNTs and the reactivities of the carboxylic groups on armchair and zigzag CNTs [10] have been reported. In recent years, the trend in the CNT research has been to calculate the aromaticities of these structures too [11].

Small atomic clusters often exhibit structures and properties that are remarkably different from those of their bulk counterparts. For example, boron nitride has a wide range of attractive properties, such as high-temperature stability, low dielectric constant, large thermal conductivity, and oxidation resistance, leading to a number of potential applications as structural or electronic materials [12–15]. Boron nitride (BN) nanostructured materials with a bandgap energy (E_g) of $\sim$6 eV and a lack of magnetism are also expected to show various electronic, optical and magnetic properties, such as Coulomb blockade, photoluminescence, and superparamagnetism [16]. Several studies have been made on BN nanomaterials such as BN nanotubes [17–20], BN nanocapsules [20], BN nanoparticles [21, 22] and BN clusters [16], which are expected to be

useful as electronic devices, high heat-resistance semiconductors and insulator lubricants. Some BN nanocage clusters have also been predicted theoretically [23, 24], and BN clusters with sizes of ~ 1 nm have been observed only by high-resolution electron microscopy [16, 25] (HREM), which is a powerful method for direct observing the atomic structures of advanced materials [26, 27]. BN metallofullerenes, which showed that it was possible to have metal atoms inside $B_{36}N_{36}$ clusters, were also identified using HREM [16, 28]. However, mass spectrum analysis has been mandatory in order to determine the existence of BN cage clusters and BN metallofullerenes.

Recently, a mass spectral analysis of $B_{24}N_{24}$ clusters was reported [29]. The geometries and stabilities of $(BN)_n$ ($n = 4$–30) have been studied by many research groups [30–34]. Fowler et al. [35] found that $B_{12}N_{12}$, $B_{16}N_{16}$ and $B_{28}N_{28}$ stand out as ''magic'' BN fullerenes, and $B_{12}N_{12}$ appears to be more stable than the others. The favored $B_{12}N_{12}$ [36, 37] cluster has a structure based on decoration of the truncated octahedron in which all *B* vertices remain equivalent, as do all *N*. The overall symmetry of the decorated structure is T_h, compared with the O_h symmetry of the unsubstituted bare framework. The six quadrilaterals are rhomboidal and separated by hexagonal rings.

Sheichenko et al. [38] have studied the electronic properties of B_nN_n ($n = 12$, 24, 60) fullerene-like molecules using semiempirical and ab initio methods. The third-order nonlinear optical polarizabilities for $B_{12}N_{12}$, $B_{24}N_{24}$ and $B_{36}N_{36}$ clusters were calculated by employing ab initio time-dependent density functional theory combined with a sum-over-states method (SOS//TDDFT) [39]. The electronic structure, vibrational stability, infra-red, and Raman spectra of $B_{24}N_{24}$ cages have also been studied using electron density-functional calculations [40]. The possibility of hemispherical caps of boron nitride nanotubes has also been reported by Zope et al. [41].

The calculation of nuclear magnetic resonance (NMR) parameters using ab initio techniques has become a major and powerful tool in the investigation of molecular structure. The ability to quickly evaluate and correlate the magnitude and orientation of the chemical shielding anisotropy (CSA) tensor with variations in bond angles, bond length, local coordination number and nearest-neighbor interactions has seen a number of recent applications in the investigation of molecular structure [42]. We are interested in utilizing ab initio computational techniques to look at how variations in the molecular structure impact the resulting ^{11}B and ^{14}N NMR and NQR observables. Magnetic nuclei chemical shielding tensors for nuclei with fractional spin like ^{11}B and ^{14}N reveal very valuable information about the physical environment and especially the electrostatic environment around the nuclei. However, because of the complex electrostatic environment of the nanocages, practical spectrometry that directly explores the electrostatic environment around the nucleus is difficult. Therefore, quantum calculations play a very important role in measuring the NMR parameters of nanocages. Nuclear quadrupole resonance (NQR) spectroscopy, which is applied to quadrupole nuclei, is among the most versatile and insightful techniques used to investigate the physical properties of matter [43]. Quadrupole nuclei are those that have nuclear spin angular momentum greater than one-half ($I > 1/2$), e.g., ^{11}B and ^{14}N. The quadrupole coupling constant (χ) and the asymmetry parameter (η) can be determined via quantum chemical calculations of the electric field gradient (EFG) tensors. χ is proportional to the interaction energy between the nuclear electric quadrupole moment (eQ) and the EFG tensors at the quadrupole nuclei sites [44].

Another important measurable parameter is the asymmetry parameter (η), meaning the deviation of the EFG tensors from cylindrical symmetry at quadrupole nuclei sites. The EFG tensors are very sensitive to the electrostatic environment and can reveal new aspects of these properties in $B_{24}N_{24}$ fullerenes. Computationally, the calculated EFG tensors are proportional to χ and η; therefore, quantum chemical calculations permit the evaluation of parameters measurable with NQR. The present computational work investigates the electrostatic properties of $B_{24}N_{24}$ fullerenes systematically. Therefore, the nuclear magnetic shielding tensors and the EFG tensors were calculated in order to evaluate the NMR (σ_{iso}) and NQR parameters (χ and η) (Tables 1, 2, 3, 4, 5, 6) of ^{11}B and ^{14}N as a first prediction for $B_{24}N_{24}$ fullerenes (Figs. 1, 2, 3), thus indicating how the electronic structure properties of these $B_{24}N_{24}$ cages are influenced by structural changes. To the best of our knowledge, no data are currently available on χ for the considered $B_{24}N_{24}$ cages or any similar $(BN)_n$ cluster structures in the literature; therefore, the present work evaluates the B-11 and N-14 chemical shieldings (σ_{iso}) and quadrupole coupling constant parameters (χ) as a first prediction for $B_{24}N_{24}$ fullborenes.

Results and discussion

NMR parameters

NMR parameters of ^{14}N and ^{11}B (σ_{iso}) in the geometrically optimized $B_{24}N_{24}$ models were evaluated by calculating the nuclear magnetic shielding tensors at the level of the B3LYP DFT method and the 6-311++G^{**} standard basis set. The results are shown in Tables 1, 2 and 3. The ab initio method utilized in the present study presumes the selection of isolated clusters for the actual calculations of isotropic chemical shielding parameters (σ_{iso}) and ignores

Table 1 GIAO-calculated chemical shieldings for a $B_{24}N_{24}$ cage with optimized S_8 symmetry

^{11}B nuclei		^{14}N nuclei	
ID[a]	σ_{iso}(ppm)	ID	σ_{iso} (ppm)
1	67	2	100
3	74	4	121
5	67	7	121
6	67	8	121
9	67	11	121
10	75	14	101
12	75	15	121
13	67	18	100
16	67	19	121
17	67	21	122
20	75	22	101
23	67	25	121
24	67	26	100
27	75	28	121
29	67	31	121
30	67	32	121
33	67	35	121
34	75	38	101
36	75	39	121
37	67	42	100
40	67	43	121
41	67	45	121

See Fig. 4 for details

[a] The ID number corresponds to the label of the individual B or N atom in the corresponding figure

Table 2 GIAO-calculated chemical shieldings for a $B_{24}N_{24}$ cage with optimized S_4 symmetry

^{11}B nuclei		^{14}N nuclei	
ID	σ_{iso}(ppm)	ID	σ_{iso} (ppm)
1	68	3	91
2	68	4	91
11	67	5	131
12	67	6	106
13	67	7	89
14	67	8	106
15	67	9	131
16	67	10	88
17	65	21	123
18	72	22	97
19	65	23	123
20	72	24	97
25	65	26	98
27	67	28	89
29	67	30	89
31	67	33	92
32	68	34	132
35	67	37	132
36	68	38	92
39	72	40	123
41	72	42	123
43	65	44	98
45	67	46	106
47	67	48	106

See Fig. 5 for details

interactions among adjacent clusters. In this manner it is possible to obtain discrete clusters for the geometry optimization and chemical shielding calculations. As the Tables 1, 2 and 3 show, the main difference between boron and nitrogen nuclei is the nonbonding electron pair in the nitrogen valence shell, whereas the boron atom has a lack of valence shell electrons. This makes boron atoms rather acidic and nitrogen rather basic, resulting in a difference in behavior for these nuclei in boron nitride nanocages. Nitrogen nuclei have greater isotropic chemical shielding than boron nuclei. This phenomenon means that boron and nitrogen adopt different roles in $B_{24}N_{24}$ fullborenes. As we can see from Table 1, the most stable $B_{24}N_{24}$ with the S_8 point group consists of two lines with chemical shieldings of $\sim$67 and 75 ppm for boron atoms and two lines with chemical shieldings of $\sim$121 and 100–101 ppm for nitrogen atoms. In Table 2, peaks at $\sim$65–68 and 72 ppm are assigned to boron atoms, and peaks at $\sim$89–92, 97–101, 106 and 123 ppm reflect the chemical shieldings of nitrogen atoms in the S_4 $B_{24}N_{24}$ cage. The results of our calculations, as shown in Table 3, also predict $\sim$72–73 ppm shielding of the signals from boron atoms and $\sim$122–123 ppm chemical shielding from nitrogen atom signals in $B_{24}N_{24}$ fullborene with O symmetry.

NQR parameters

The results from NQR quantum chemical calculations of parameters (χ, η) for fully relaxed $B_{24}N_{24}$ fullborenes are shown in Tables 4, 5 and 6. Since no experimental NQR data for $B_{24}N_{24}$ fullerenes are available in the literature, the tables do not reference any experimental data for the calculated results. Comparing the χ values computed in this work with the ^{14}N and ^{11}B NQR parameters in the (4,4) BNNT calculated and reported by Hadipour et al. [45] verifies the χ values calculated in this work for $B_{24}N_{24}$ clusters. In the following, we discuss the calculated NQR parameters of ^{14}N and ^{11}B nuclei of $B_{24}N_{24}$ fullerenes. The calculated NQR parameters at the positions of ^{14}N nuclei are presented in Tables 4, 5 and 6 for the three $B_{24}N_{24}$ models, respectively. A quick look at the results from the calculations reveals that the NQR parameters vary for the nuclei; therefore, the electrostatic

Table 3 GIAO-calculated chemical shieldings for a $B_{24}N_{24}$ cage with optimized O symmetry

^{11}B nuclei		^{14}N nuclei	
ID	σ_{iso} (ppm)	ID	σ_{iso} (ppm)
1	73	3	123
2	72	4	123
5	72	8	122
6	72	9	123
7	72	10	123
12	72	11	123
13	72	16	123
14	72	17	123
15	72	18	123
20	72	19	123
21	72	24	122
22	72	25	123
23	73	26	123
27	73	28	123
29	73	31	123
30	72	32	123
33	72	34	123
36	72	35	123
38	72	37	123
39	72	40	123
41	73	42	123
44	72	43	123
45	72	46	123
48	72	47	123

See Fig. 6 for details

Table 4 The ^{14}N and ^{11}B NQR parameters for $B_{24}N_{24}$ with optimized S_8 symmetry

ID	^{14}N nuclei		ID	^{11}B nuclei	
	χ	η		χ	η
2	0.52	0.30	1	3.13	0.13
4	0.73	0.79	3	3.11	0.13
7	0.91	0.44	5	3.13	0.12
8	0.91	0.44	6	3.13	0.13
11	0.73	0.79	9	3.13	0.12
14	0.52	0.30	10	3.11	0.13
15	0.91	0.44	12	3.11	0.13
18	0.52	0.30	13	3.13	0.12
19	0.73	0.79	16	3.13	0.13
21	0.73	0.79	17	3.13	0.12
22	0.52	0.30	20	3.11	0.13
25	0.91	0.44	23	3.13	0.13
26	0.52	0.30	24	3.13	0.13
28	0.73	0.79	27	3.11	0.13
31	0.91	0.44	29	3.13	0.12
32	0.91	0.44	30	3.13	0.13
35	0.73	0.79	33	3.13	0.12
38	0.52	0.30	34	3.11	0.13
39	0.91	0.44	36	3.11	0.13
42	0.52	0.30	37	3.13	0.12
43	0.73	0.79	40	3.13	0.13
45	0.73	0.79	41	3.13	0.12
46	0.52	0.30	44	3.11	0.13
48	0.91	0.44	47	3.13	0.13

See Fig. 4 for details

environments of these three $B_{24}N_{24}$ fullborenes with different symmetries are not equivalent, although these differences are not very conspicuous. If we divide the S_8 cage—the most stable $B_{24}N_{24}$ fullborene—into two hemispheres as shown in Fig. 4, the χ values for the ^{14}N nuclei that have symmetrical positions in the cage hemispheres show absolute equivalence (Table 4; Fig. 4). We observe the same pattern for ^{11}B nuclei, but all of the ^{11}B atoms have approximately the same χ values, whatever the values of the ^{14}N nuclei. In the S_4 model of $B_{24}N_{24}$ fullborene, the χ values of ^{14}N nuclei (Table 5; Fig. 5) are more diverse than those of the ^{14}N nuclei in the S_8 model. In addition, some ^{14}N nuclei in S_4 $B_{24}N_{24}$ fullborene have bigger χ values, while some of them have smaller values, but the ^{11}B nuclei in the S_4 model do not show considerable differences in χ from those in the S_8 model. When we look at Table 6, we can see that the χ values of all of the ^{14}N and also all of the ^{11}B nuclei in the $B_{24}N_{24}$ model with O symmetry have equal values, and so the cage has a uniform electrostatic environment. Taken together, this shows that there are only small differences between the geometrical properties of these $B_{24}N_{24}$ cages, and so, because the results in Tables 4, 5 and 6 reflect the fact that the NQR parameters for these three cages are not completely similar, this indicates the sensitivity of the EFG tensors to changes in the geometrical properties in the considered $B_{24}N_{24}$ models. For more about the NQR parameters, see Tables 4, 5 and 6 and Figs. 4, 5 and 6. It is obvious that, since the N atom has a lone pair of electrons in the valence shell whereas the B atom lacks electrons in its valence shell, the NQR parameters at the sites of N nuclei differ more at different locations in the cages compared to those of the B nuclei.

Concluding remarks

The goal of this study was, for the first time, to calculate the NMR and NQR parameters at the locations of ^{14}N and ^{11}B nuclei in the three most stable $B_{24}N_{24}$ models with S_8, S_4 and O symmetries. Optimization of geometries and NMR and NQR calculations of the considered structures were also performed.

Table 5 The ^{14}N and ^{11}B NQR parameters for S_4 $B_{24}N_{24}$ with optimized S_4 symmetry

ID	^{14}N nuclei		ID	^{11}B nuclei	
	χ	η		χ	η
3	0.70	0.91	1	3.18	0.12
4	0.70	0.91	2	3.18	0.12
5	1.10	0.52	11	3.15	0.055
6	1.17	0.55	12	3.24	0.055
7	0.70	0.92	13	2.94	0.045
8	1.17	0.55	14	2.94	0.045
9	1.10	0.52	15	3.24	0.055
10	0.70	0.92	16	3.15	0.055
21	1.50	0.29	17	3.28	0.14
22	0.32	0.97	18	3.17	0.092
23	1.50	0.29	19	3.28	0.14
24	0.32	0.97	20	3.17	0.092
26	0.32	0.96	25	3.28	0.14
28	0.70	0.92	27	3.15	0.055
30	0.70	0.92	29	3.15	0.055
33	0.70	0.91	31	3.24	0.055
34	1.10	0.52	32	3.18	0.12
37	1.10	0.52	35	3.24	0.055
38	0.70	0.91	36	3.18	0.12
40	1.48	0.29	39	3.17	0.092
42	1.48	0.29	41	3.17	0.092
44	0.32	0.96	43	3.28	0.14
46	1.17	0.55	45	2.94	0.045
48	1.17	0.55	47	2.94	0.045

See Fig. 5 for details

Table 6 The ^{14}N and ^{11}B NQR parameters for $B_{24}N_{24}$ with optimized O symmetry

ID	^{14}N nuclei		ID	^{11}B nuclei	
	χ	η		χ	η
3	0.68	0.70	1	3.10	0.19
4	0.68	0.70	2	3.11	0.19
8	0.68	0.70	5	3.10	0.19
9	0.69	0.70	6	3.10	0.19
0	0.68	0.70	7	3.10	0.19
11	0.68	0.70	2	3.10	0.19
16	0.68	0.70	13	3.10	0.19
17	0.69	0.70	14	3.10	0.19
18	0.68	0.71	15	3.10	0.19
19	0.68	0.70	20	3.10	0.19
24	0.69	0.70	21	3.10	0.19
25	0.69	0.70	22	3.10	0.19
26	0.68	0.71	23	3.10	0.19
28	0.68	0.70	27	3.10	0.19
31	0.69	0.70	29	3.10	0.19
32	0.68	0.71	30	3.10	0.19
34	0.68	0.71	33	3.10	0.19
35	0.68	0.70	36	3.10	0.19
37	0.68	0.71	38	3.10	0.19
40	0.68	0.70	39	3.10	0.19
42	0.68	0.71	41	3.10	0.19
43	0.68	0.70	44	3.10	0.19
46	0.69	0.70	45	3.10	0.19
47	0.68	0.70	48	3.10	0.19

See Fig. 6 for details

All of these $B_{24}N_{24}$ cages have just squares, hexagons and octagons, and the only difference between them is the number of these polygons. The most stable isomer, S_8 has two octagons, sixteen hexagons and eight squares (see Fig. 1). The S_4 symmetry model consists of 20 hexagons and six squares (see Fig. 2), while the O symmetry cage has six octagons, eight hexagons and 12 squares (see Fig. 3). The energies of these three $B_{24}N_{24}$ isomers also only show very small differences (see Figs. 1, 2 and 3).

The calculated chemical shieldings (σ_{iso}) indicated that the ^{14}N nuclei in S_8 fullborene show approximately two peaks at around 121 and 100–101 ppm, and two peaks for ^{11}B nuclei close to 67 and 75 ppm. The components at ~89–92, 97–101, 106 and 123 ppm correspond to ^{14}N nuclei and at ~65–68 and 72 ppm to ^{11}B nuclei in the S_4 model, so this model shows four peaks for ^{14}N and two peaks for ^{11}B nuclei, respectively. The model with O symmetry shows one peak at ~122–123 ppm which is attributed to ^{14}N nuclei and one peak at ~72–73 ppm which reflects the chemical shielding of ^{11}B nuclei. As we can see, NMR quantum calculations are a useful tool for studying the structural features of three different $B_{24}N_{24}$ models, since the positions of the NMR signals in each model are well reflected in the NMR chemical shieldings. The predicted NMR parameters may aid experimenters in identifying the structure of $B_{24}N_{24}$. In addition, we can see that the nuclear magnetic shielding tensors of ^{14}N nuclei display substantial sensitivity to structural changes, while ^{11}B nuclei do not show this feature.

The calculated NQR parameters revealed that the electrostatic environments of the three $B_{24}N_{24}$ clusters are as different as their structures. The χ values of the ^{11}B nuclei in all the cages do not show tangible changes, whereas the χ values of the ^{14}N nuclei do show variations. As the NQR calculations show, the electrostatic environment of the isomer with O symmetry is homogeneous throughout the cluster, but the S_8 and S_4 cages do not exhibit this characteristic. However, we can divide S_8 cage into two hemispheres which have identical electrostatic environments, as we discussed earlier. The χ values of the ^{11}B nuclei in all of the cages are greater than of

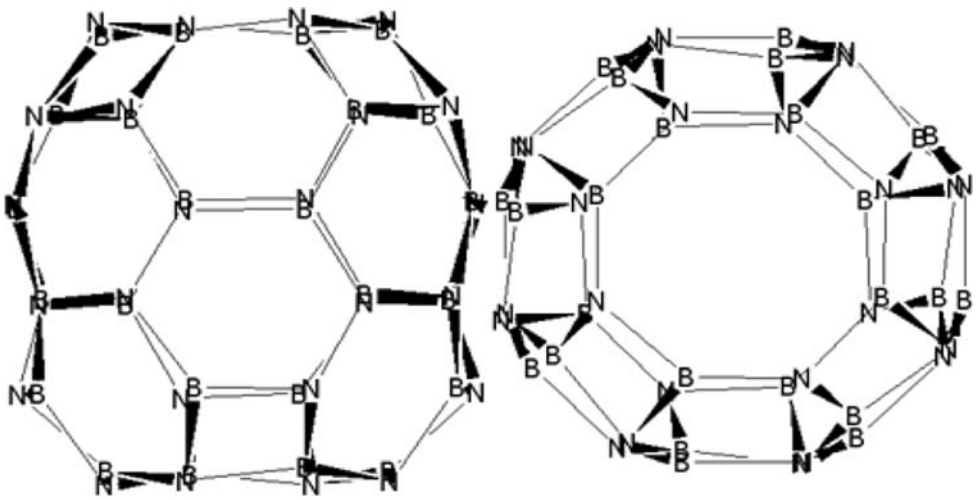

Fig. 1 Two different views of $B_{24}N_{24}$ with optimized S_8 symmetry

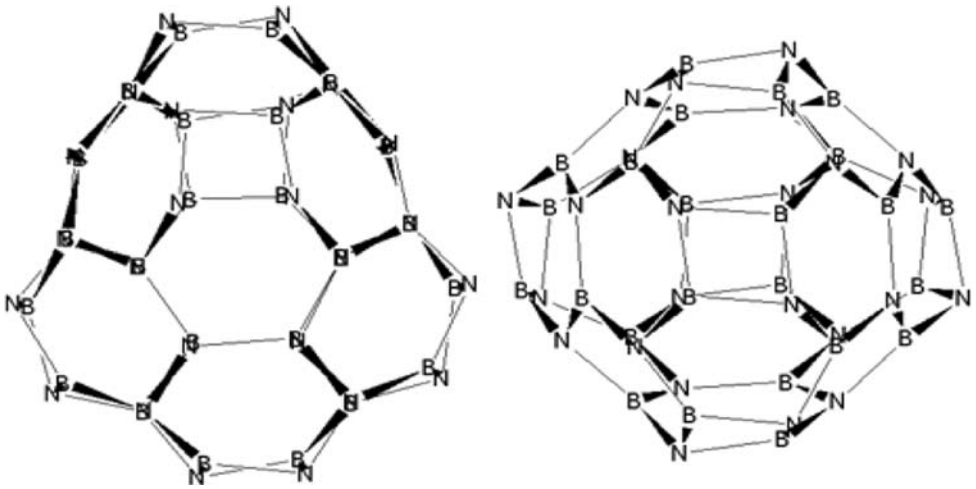

Fig. 2 Two different views of $B_{24}N_{24}$ with optimized S_4 symmetry

those of the ^{14}N nuclei. The calculated NQR parameters will play a key role when studying the interactions of atoms and molecules with the clusters, which are important in catalysis as well as in the development of cluster-based materials.

Computational methods and details

In our investigation, the three candidate structures were a round cage with an octahedral O symmetry, a cage with S_4 symmetry, and a cage with S_8 symmetry, which combines

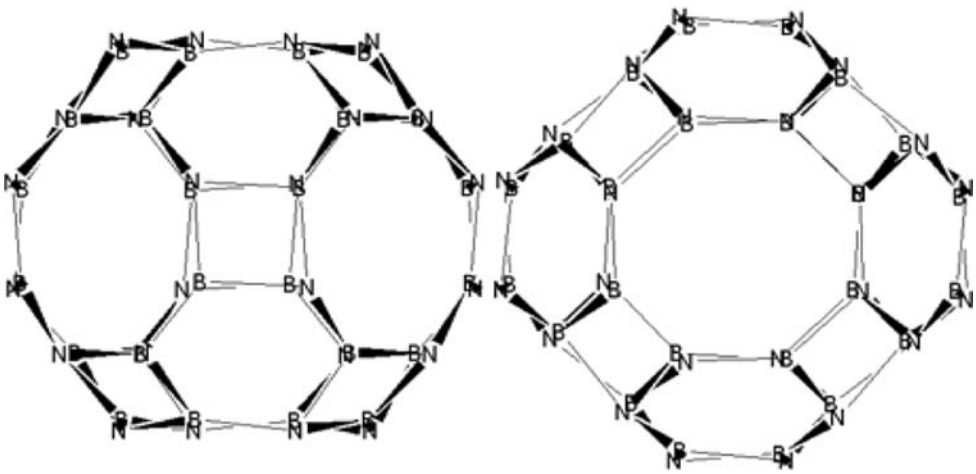

Fig. 3 Two different views of $B_{24}N_{24}$ with optimized O symmetry

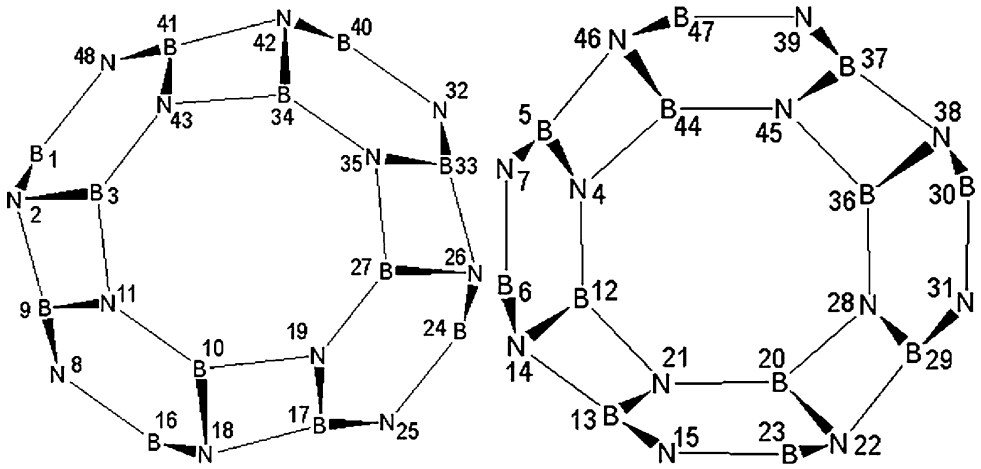

Fig. 4 Two halves of the $B_{24}N_{24}$ with optimized S_8 symmetry

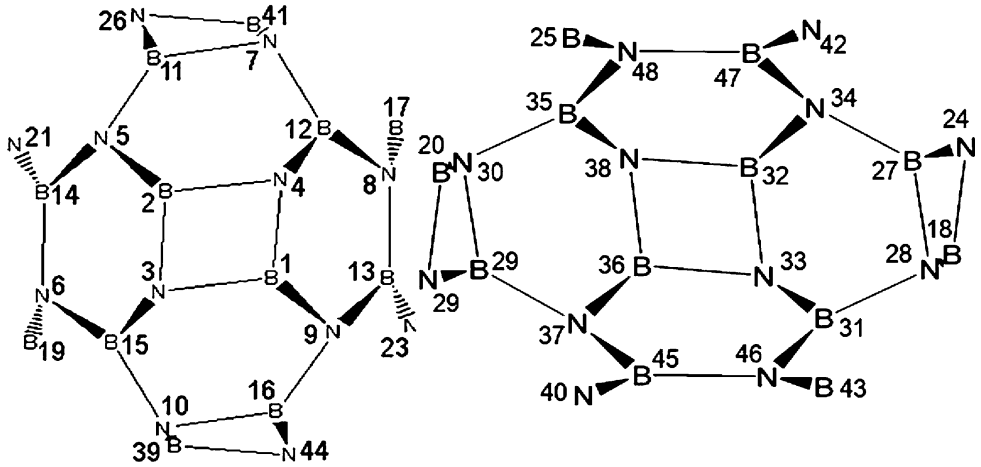

Fig. 5 Two halves of the $B_{24}N_{24}$ with optimized S_4 symmetry

the caps of the (4,4) borone nitride nanotube and contains two extra squares and octagons that are considered in the quantum chemical calculations (Figs. 1, 2, 3). The gauge-including atomic orbital (GIAO) method [46] at the level of DFT was applied to the considered BN fullerenes using the Gaussian 98 [47] software package. The most commonly used methods of calculating chemical shifts are the individual gauge for localized orbitals (IGLO) method, the

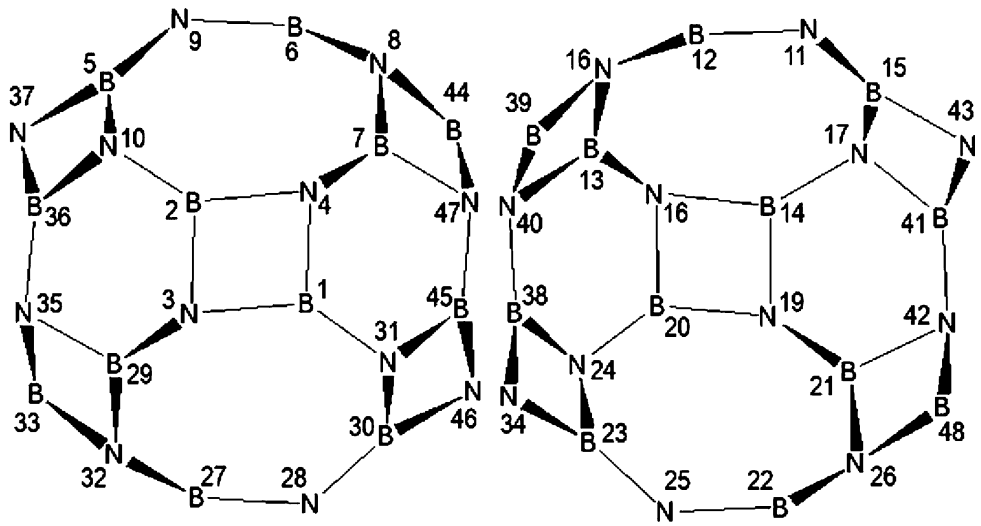

Fig. 6 Two halves of the $B_{24}N_{24}$ with optimized O symmetry

localized orbital/local origin (LORG) method, and the gauge-independent or -invariant or -including atomic orbital (GIAO) method. Reviewing Chemical Abstracts (for works published between 1987 and 2001) for the mentioned methods reveals that GIAO is the method most commonly used to calculate absolute shieldings [48].

First, the considered model systems were optimized using the B3LYP exchange-functional method [49, 50] and the 6-311G** standard basis set. Secondly, quantum chemical calculations were carried out for the geometrical optimized models using the B3LYP method and the 6-311++G** standard basis set. There were five d-type Gaussian polarization functions on each non-hydrogen atom and three p-type polarization functions on each hydrogen atom in the large Pople valence triple-zeta 6-311G** and 6-311++G** [51] basis sets. In the second basis set, 6-311++G**, diffuse functions are on all atoms indicated by two pluses [52], to evaluate the ^{14}N and ^{11}B NMR and NQR parameters (see Tables 1, 2, 3 4, 5, 6). These quantum chemical calculations do not directly yield experimentally measurable NMR and NQR parameters. The quantum chemistry calculations were adapted to reproduce reliable NMR properties [53, 54]. The NMR parameter is the isotropic value (or trace), σ_{iso}, of the shielding tensor, which is defined as shown in Eq. 1:

$$\sigma_{iso} = 1/3(\sigma_{11} + \sigma_{22} + \sigma_{33}) \quad (1)$$

The chemical shielding tensors obtained from the calculations are in the principal axis system (PAS) ($\sigma_{11} > \sigma_{22} > \sigma_{33}$). The NQR parameters are the nuclear quadrupole coupling constant χ and the asymmetry parameter η. However, Eqs. 2 and 3 are used to relate the calculated EFG tensors to their associated experimentally measurable parameters:

$$\chi(\mathrm{MHZ}) = e^2 Q q_{zz}/h \quad (2)$$

$$\eta = |q_{xx} - q_{yy}/q_{zz}| \quad 0 < \eta < 1 \quad (3)$$

Here, χ is the interaction energy for the nuclear electric quadrupole moment eQ and the EFG tensors, whereas η is a measure of the deviation of the EFG tensors from cylindrical symmetry at the sites of the quadrupole nuclei. Quadrupole nuclei are those that have a nuclear spin angular momentum of greater than one-half ($I > 1/2$). The EFG tensor eigenvalues were calculated in the principal axis system (PAS) using the relation $|q_{zz}| > |q_{yy}| > |q_{xx}|$. The standard Q values reported by Pyykkö [55] were employed in Eq. 2: $Q(^{14}\mathrm{N}) = 20.44$ mb and $Q(^{11}\mathrm{B}) = 40.59$ mb. Tables 4, 5 and 6 show the calculated NQR parameters for ^{14}N and ^{11}B nuclei in the three candidate models.

References

1. Kroto HW, Heath JR, O'Brien SC, Smalley RE (1985) Nature 318:162
2. Dresselhaus M, Dresselhaus G, Eklund PC (1996) Science of fullerenes and carbon nanotubes. Academic, New York
3. Iijima S (1991) Nature 354:56
4. Oku T, Hirano T, Kuno M, Kusunose T, Niihara K, Suganuma K (2000) Mater Sci Eng B 74:206
5. Berber S, Kwon YK, Tomanek D (2000) Phys Rev Lett 84:4613
6. Mintmire JW, Dunlap BI, White CT (1992) Phy Rev Lett 68:63
7. Saito R, Fujita M, Dresselhaus MS, Dresselhaus GR (1992) Phy Rev B 46:1804
8. Hamada N, Sawada S, Oshiyama A (1992) Phys Rev Lett 68:1579
9. Matsuo Y, Tahara K, Nakamura E (2003) Org Lett 18:3181
10. Basiuk VA (2002) Nano Lett 2:835
11. Linert W, Lukovits I (2007) J Chem Inf Model 47:887–890
12. Paine RT, Narula CK (1990) Chem Rev 90:73
13. Oku T, Hirano T, Kuno M, Kusunose T, Niihare K, Suganuma K (2000) Mater Sci Eng B 74:206
14. Oku T, Kuno M, Kitahara H, Nartia I (2001) Int J Inorg Mater 3:597
15. Kokado S, Harigaya K (2003) Synth Metals 135–136:745
16. Oku T, Kuno M, Kitahara H, Narita I (2001) Int J Inorg Mater 3:597
17. Chopra NG, Luyken RJ, Cherrey K, Crespi VH, Cohen ML, Louie SG, Zettl A (1995) Science 269:966
18. Mickelson W, Aloni S, Han W-Q, Cumings J, Zettl A (2003) Science 300:467
19. Narita I, Oku T (2002) Solid State Commun 122:465
20. Narita I, Oku T (2003) Diamond Relat Mater 12:1146
21. Oku T, Hiraga K, Matsuda T, Hirai T, Hirabayashi M (2003) Diamond Relat Mater 12:1138
22. Oku T, Hiraga K, Matsuda T, Hirai T, Hirabayashi M (2003) Diamond Relat Mater 12:1918
23. Alexandre SS, Mazzoni MSC, Chacham H (1999) Appl Phys Lett 75:61
24. Pokropivny VV, Skorokhod VV, Oleinik GS, Kurdyumov AV, Bartnitskaya TS, Pokropivny AV, Sisonyuk AG, Sheichenko DM (2000) J Solid State Chem 154:214
25. Golberg D, Bando Y, St!ephan O, Kurashima K (1998) Appl Phys Lett 73:2441
26. Oku T (2001) J Ceram Soc Jpn 109:S17
27. Oku T (2004) J Phys Chem Solids 65:363
28. Oku T, Kuno M, Narita I (2002) Diamond Relat Mater 11:940
29. Oku T, Nishiwaki A, Narita I, Gonda M (2003) Chem Phys Lett 380:620
30. Sun M-L, Slanina Z, Lee S-L (1995) Chem Phys Lett 233:279–283
31. Wu H-S, Jiao H (2004) Chem Phys Lett 386:369–372
32. Batista RJC, Mazzoni MSC, Chacham H (2006) Chem Phys Lett 421:246–250
33. Mileev MA, Kuzmin SM, Parfenyuk VI (2006) J Struct Chem 47(6):1016–1021
34. Wu H-S, Jiao H (2006) J Mol Model 12:537–542
35. Seifert G, Fowler RW, Mitchell D, Porezag D, Frauenheim T (1997) Chem Phys Lett 268:352
36. Strout DL (2000) J Phys Chem A 104:3364
37. Strout DL (2001) J Phys Chem A 105:261
38. Sheichenkov DM, Pokropivny AV, Pokropivny VV (2000) Semicond Phys Quant Electron Optoelectron 3(4):545–549
39. Lan Y-Z, Cheng W-D, Wu D-S, Li X-D, Zhang H, Gong Y-J, Shen J, Li F-F (2005) J Mol Struct (Theochem) 730:9–15

40. Zope RR, Baruah T, Pederson MR, Dunlap BI (2004) Chem Phys Lett 393:300–304
41. Zope RR, Dunlap BI (2004) Chem Phys Lett 386:403–407
42. Facelli JC, de Dios AC (eds)(1999) Modeling NMR chemical shifts, gaining insights into structure and environment. American Chemical Society, Washington, DC
43. Das TP, Han EL (1958) Nuclear quadrupole resonance spectroscopy. Academic, New York
44. Bailey WC (2000) Chem Phys 252:257
45. Mirzaei M, Hadipour NL (2008) Phys E 40:800–804
46. Ditchfield R, Hehre WJ, Pople JA (1972) Self-consistent molecular-orbital methods. IX. An extended Gaussian-type basis for molecular-orbital studies of organic molecules. J Chem Phys 54:724–728
47. Frisch MJ, Trucks GW, Schlegel HB, Scuseria GE, Robb MA, Cheeseman JR, Zakrzewski VG, Montgomery JA Jr, Stratmann RE, Burant JC, Dapprich S, Millam JM, Daniels AD, Kudin KN, Strain MC, Farkas O, Tomasi J, Barone V, Cossi M, Cammi R, Mennucci B, Pomelli C, Adamo C, Clifford S, Ochterski J, Petersson GA, Ayala PY, Cui Q, Morokuma K, Malick DK, Rabuck AD, Raghavachari K, Foresman JB, Cioslowski J, Ortiz JV, Baboul AG, Stefanov BB, Liu G, Liashenko A, Piskorz P, Komaromi I, Gomperts R, Martin RL, Fox DJ, Keith T, Al-Laham MA, Peng CY, Nanayakkara A, Gonzalez C, Challacombe M, Gill PMW, Johnson B, Chen W, Wong MW, Andres JL, Gonzalez C, Head-Gordon M, Replogle ES, Pople JA (1998) Gaussian 98, revision A.7. Gaussian, Inc., Pittsburgh, PA
48. Alkorta I, Elguero J (2003) Struct Chem 14(4):337
49. Becke AD (1993) J Chem Phys 98:5648
50. Lee C, Yang W, Parr RG (1988) Phys Rev B 37:785
51. Krishnan R, Binkley JS, Seeger R, Pople JA (1980) J Chem Phys 72:650
52. Clark T, Chandrasekhar J, PRv Schleyer (1983) J Comp Chem 4:294
53. Schindler M, Kutzelnigg W (1983) J Am Chem Soc 105:1360
54. Fleischer U, Kutzelnigg W, Bleiber A, Sauer J (1993) J Am Chem Soc 115:7833
55. Pyykkö P (2001) Mol Phys 99:1617